J Mol Model (2013) 19:4099–4109
DOI 10.1007/s00894-012-1711-x

ORIGINAL PAPER

Electronic structure theory based study of proline interacting with gold nano clusters

Sandhya Rai · Harjinder Singh

Received: 15 October 2012 / Accepted: 26 November 2012 / Published online: 21 December 2012

Abstract Interaction between metal nanoparticles and biomolecules is important from the view point of developing and designing biosensors. Studies on proline tagged with gold nanoclusters are reported here using density functional theory (DFT) calculations for its structural, electronic and bonding properties. Geometries of the complexes are optimized using the PBE1PBE functional and mixed basis set, i.e., 6-311++G for the amino acid and SDD for the gold clusters. Equilibrium configurations are analyzed in terms of interaction energies, molecular orbitals and charge density. The complexes associated with cluster composed of an odd number of Au atoms show higher stability. Marked decrease in the HOMO-LUMO gaps is observed on complexation. Major components of interaction between the two moieties are: the anchoring N-Au and O-Au bond; and the non covalent interactions between Au and N-H or O-H bonds. The electron affinities and vertical ionization potentials for all complexes are calculated. They show an increased value of electron affinity and ionization potential on complexation. Natural bond orbital (NBO) analysis reveals a charge transfer between the donor (proline) and acceptor (gold cluster). The results indicate that the nature of interaction between the two moieties is partially covalent. Our results will be useful for further experimental studies and may be important for future applications.

Keywords AIM · Electron affinity · Gold cluster · Ionization potential · NBO · Proline

Electronic supplementary material The online version of this article (doi:10.1007/s00894-012-1711-x) contains supplementary material, which is available to authorized users.

S. Rai · H. Singh (✉)
International Institute of Information Technology,
Hyderabad, India
e-mail: laltu@iiit.ac.in

Introduction

Nano metal clusters are known to have size-dependent electronic and optical properties, ranging from metal like to molecule like, such as single-electron charging and quantum size effects [1]. Hence, they are fundamentally interesting and in many cases are found to have useful technological applications [2–4]. Conjugated gold nanoparticles have attracted much attention in chemistry and material science because of their property of self-assembly, in developing potential miniature devices [5–10]. Gold nanoparticles attract interest also because their optical, catalytic and electronic properties characteristically depend on the conjugating particles that form complexes with gold [11–13]. An added interest in gold nanoclusters is due to the recent experimental and theoretical discoveries of large planar gas-phase gold clusters [13, 14]. The occurrence of planar metal clusters of this size is unprecedented, and their stability is attributed to strong relativistic bonding effects in gold that reduce the s–d energy gap, thus inducing hybridization of the atomic 5d–6s levels and causing overlap of the 5d shells of the neighboring atoms in cluster [13, 15, 16]. Huang et al. have reported preferential physisorption of Argon on a 2D gold cluster over a 3D cluster of same size [17].

Miniaturization of structures has created a platform for nano-biomedical research as well [18–20]. Tagging of noble metal nanoparticles to biomolecules is well investigated both theoretically as well as experimentally. Yu et al. have found that oligoDNA-protected silver clusters get covalently conjugated to proteins and primary antibodies without significant interference of either biological function or nanocluster photophysics [21]. Upert et al. have shown the size controlled synthesis of silver nanoparticles using oligoproline scaffolds [22]. It has also been shown that low nuclearity of silver clusters are highly attractive for application as

optical probes for biomolecules, due to their low toxicity and very small size [23, 24]. The tagging of dipeptides with silver nanoclusters reduces the conformational flexibility of the dipeptide thereby inducing transitions between secondary structures [23]. The nontoxic and biocompatible nature of gold nanoparticles has put them on the center stage for designing therapeutic drug delivery vehicles [25]. Pal et al. have suggested that attachment of AuNP to peptides does not change the antimicrobial activity too much but the cytotoxicity of the peptides is decreased significantly [26]. It has been found that interaction between biomolecules and gold nanoparticles has potential application in the field of biosensors, biodiagnostics, etc. [27–30]. An example is a recent study on Tryptophan tagged with a single gold cation recording a strong absorption band in the visible spectral region attributed to charge-transfer excitations [31]. The assembly of proteins on gold surface has a large number of applications in the field of biotechnology ranging from protein detection to cancer therapy. It has also been found that serum proteins become associated with nanoparticles in biological medium and form a protein 'corona', which defines the identity of the particles within the biological system thus making the protein-nanoparticle interaction particularly interesting [32]. Imaging of cells and immunolabeling using gold nanoparticles is another area of research, which is extensively being investigated these days [33]. Nanoparticle interaction with plasma protein is found to activate the protein and results in inflammatory responses. Immunoassays based on gold nanoparticle interaction with antibody conjugates and their antigens have also been developed recently [34].

Proline is a unique amino acid in the sense that the amine nitrogen is bound to two alkyl groups instead of one, and hence is an example of secondary nitrogen group. This results in conformational rigidity hence providing some peculiar properties to this amino acid. Proline functions as a universal antioxidant and is found to provide effective protection against H_2O_2 stress [35]. It also functions as an osmoprotectant [36].

We have employed methods based on the density functional theory (DFT) to determine the nature of interaction between proline and nanogold (Au_n, where n ranges from 3 to 13) clusters. Studies are carried out on L-proline. The interaction has been described in terms of equilibrium configurations, interaction energies, and HOMO-LUMO gaps. Natural bond orbital (NBO) analysis has been performed to quantify the charge transfer interactions. Atoms-in-molecules (AIM) theory has been applied to better understand the nature of bonding between proline and gold clusters. Calculations of vertical ionization energy and electron affinity have also been done in order to study the electron transfer in these systems. Our results can be useful for future studies based on designing new materials involving these kinds of interactions.

Computational details

The benchmark study of Zhao and Truhlar [37, 38], concerning DFT performances on describing nonbonded interactions says that the B3LYP hybrid density functional, widely accepted as the standard DFT method, describes the nonbonded interactions rather poorly, while the PBE1PBE functional is one of the best methods describing these types of interactions [39]. Therefore all the structures were optimized using the exchange correlation functional proposed by Perdew, Burke and Ernzerhof (PBE1PBE) functional [40–42]. Stuttgart-Dresden 11-electron ECP, designated as SDD was used for gold [43–46]. These energy-consistent ECPs work within the relativistic Dirac-Fock theory and significantly remove the spin contamination. For other atoms Pople's 6-311++G split-valence basis set was used [47–50]. The initial coordinates of gold clusters were generated using GaussView [51]. These initial structures were based on earlier data reported by Hakkinen et al. [13], on bond distances and angles. Based on their proposed geometries, the input structures were made and then further optimized. The initial geometries of the complexes were generated by placing the gold clusters near the active site of proline, i.e., amine terminal and the carboxyl terminal. The harmonic vibrational frequencies and the gradients were calculated analytically. Real frequencies were obtained for all the optimized structures. The binding energies reported are zero-point vibrational energy (ZPVE) corrected. All the wave functions obtained for the optimized geometries were checked for stability. The interaction energies (E_{int}) were calculated using the following equation:

$$E_{int} = E_{complex,n} - \left[E_{proline} + E_{Au,n}\right], \quad (1)$$

where $E_{complex,\ n}$ is the ZPVE corrected electronic energy of the complex, n refers to number of Au atoms in the cluster and $E_{proline}$ and $E_{Au,n}$ are the ZPVE corrected electronic energies of uncomplexed proline and cluster, respectively. The NBO analysis [52] was performed on these complexes to examine all possible stabilizing interactions. Interactions between filled Lewis and empty non-Lewis orbitals are determined and energies of second order stabilization, $E^{(2)}$ [53], due to transfer of electron cloud from donor NBO(i) to acceptor NBO(j) are obtained using the equation:

$$E^{(2)} = q_i \left[\frac{(F(i,j))^2}{E_j - E_i}\right], \quad (2)$$

where q_i is donor orbital occupancy, E_i and E_j are energies of the orbitals i, j respectively, and F(i,j) is the off diagonal NBO

Fock matrix element. AIM analysis was performed with AIMAll package [54] to calculate the properties of bond critical points (BCPs). Vertical electron affinity ($EA_{vertical}$) and ionization potential ($IP_{vertical}$) were calculated using Eqs. 3 and 4, respectively:

$$EA_{vertical} = E_{total} - E_{anion} \quad (3)$$

$$IP_{vertical} = E_{cation} - E_{total}, \quad (4)$$

where E_{total} is the total energy of the complex, E_{anion} is the energy when one electron is added to the system and E_{cation} is the energy when one electron is removed from the system. All the calculations are performed using Gaussian 09 suite of programs, [55], and the molecular orbitals were plotted using the GaussView program [51].

Results and discussion

Geometry of proline-Au_n complexes

The interatomic interactions can be basically of two types: bonded and non-bonded. The bonded interactions include ionic, covalent, metallic and partial bond interactions, whereas, the non-bonded interactions include charge transfer, dipolar, hydrogen bonding and dispersion interactions. All the complexes that have been studied in this article are charge transfer complexes and there exists no covalent bonding between the donor and the acceptor. Optimization of clusters showed that the average Au-Au bond length falls in the range of 2.58–2.90$\mathring{A}$ (Fig. S1 of supporting information). These values are in agreement with the previously reported structures by Häkkinen et al. [13]. Active sites of proline are rich in electrons and will be able to donate the electron density to the empty 5d and 6s orbitals of gold. Owing to relativistic effects, gold has a high electron affinity which explains its high propensity to accept the electrons [15, 56]. The optimized geometries of proline tagged with gold nanoclusters, where the size of gold nanoclusters is varied from 3 to 13 are shown in Fig. 1.

In line with the observations made by earlier groups [57, 58], it is evident from Fig. 1 that there is a monodentate interaction from the amine terminal, where as the carboxyl group shows a bidentate type of interaction with the only exception of complex with Au_9 (Fig. 1.7b). The bidentate interaction in particular, involves the formation of a non conventional hydrogen bond between the gold cluster and the hydroxy group (Au···OH). Here, the gold cluster is found to act as a proton acceptor also, an observation reported in earlier works [57–59]. The geometrical features of all the optimized species have been shown in Table 1. The coordinates of the optimized geometries can be found in supporting information Table S1(a-v). It is evident from Fig. 1 that the distance between the anchoring bonds falls in the range of 2.17–2.31 Å for interaction from the amine terminal, and 2.21–3.30 Å for interaction from the carboxyl terminal. A general observation is that, as the cluster size is increased, the anchoring bond length also increases for both the terminals. It is evident from Table 1 that the corresponding N-H bond length is increased in case of interaction from the amine terminal. A red shift in N-H frequency is also observed for all the cases, but this shift is not found to be directly proportional to the interaction energy. This is because the N-H is also involved in an intramolecular hydrogen bonding interaction with the carboxyl group. For larger clusters (Au_{11-13}) this bonding gets strengthened, accounting for greater values for the N-H stretching. A similar behavior is also observed for the C = O bond during the interaction from the carboxyl terminal, but the single bond C-O is found to develop a double bond character and thereby a shortening of its length is seen in all complexes. This has also been confirmed by the blue shift in the IR frequency for C-O and a red shift in the other two cases (Table 1). In general, a decrease in magnitudes of $\angle C\text{-}N\text{-}C\alpha$ and $\angle C\alpha$-N-H is observed, going toward a pyramidal geometry with nitrogen at the vertex. Traditional hybridization arguments suggest that increase of charge by nitrogen will lead to sp^3 hybridization and a more pyramidal geometry. A special case is of interaction of carboxyl end of proline with Au_9. This is the only case where a simultaneous interaction from amine and carboxyl terminal is taking place. A red shift is observed for both N-C and C-O bonds. No hydrogen bond is observed in this case but the geometry around nitrogen is even more pyramidal, with $\angle C\alpha$-N-H exactly 109.4°. This may be due to an increase of charge by nitrogen leading to a sp^3 hybridization.

Energetics

The ZPVE corrected interaction energies are shown in Table 2.

One notable feature is that the E_{int} is higher for interaction from the amine terminal. This has also been reported in earlier works of Pakiari and Xie et al. [57, 59]. The only exception to this is for Au_9 complex, where there is a higher interaction from the carboxyl end. Rather it is interacting from both ends simultaneously, resulting in a stronger interaction. Figure 2 represents the HOMO orbital of uncomplexed proline, which is mostly localized on the amine nitrogen.

So, in accordance with the frontier molecular orbital (FMO) theory, any external electrophile will have a greater tendency to bind to proline via amine terminal. Also, nitrogen in proline is a secondary amine and hence more basic.

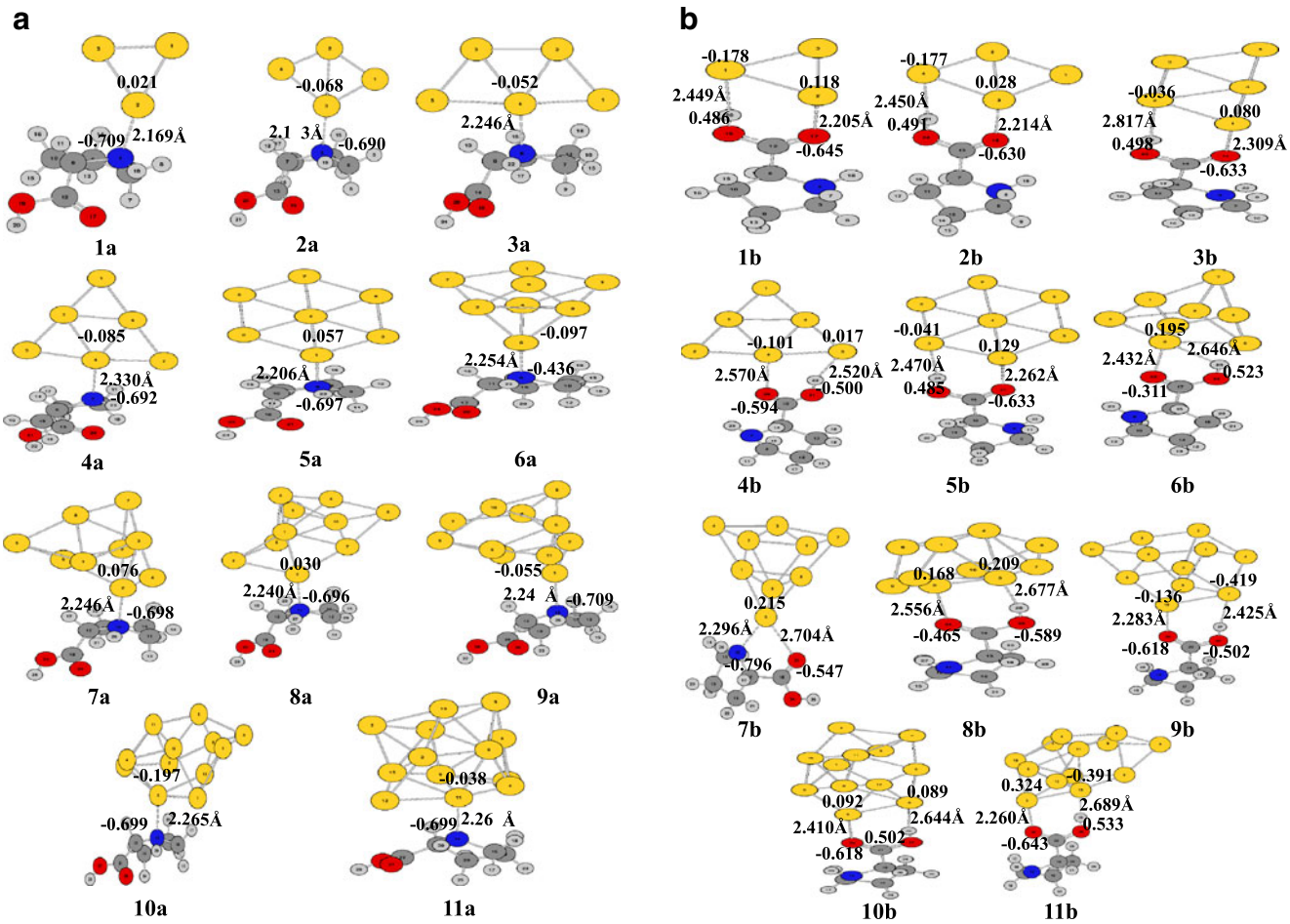

Fig. 1 Optimized structures of complexes for interaction taking place from the amine end and carboxyl end; (**a**) refers to interaction from amine terminal and (**b**) refers to interaction from carboxyl terminal. The *numbers* represent the distance between the anchoring bonds and the natural charges over important active centers

Nitrogen is less electronegative than oxygen making it a better nucleophile. So the electron donating capacity of amine terminal is higher than that of the carboxyl terminal. The higher nucleophilicity of amine terminal is also depicted in Fig. 3, which shows the molecular electrostatic potential mapped over an isodensity surface. We find a more negative potential near the amine end and hence it is more prone to an electrophilic attack by the gold cluster.

In general, we find higher interaction energy for odd numbered clusters with the only exception of complex with Au_4. When we look at the binding energies of uncomplexed clusters (Table 2), we find higher binding energies for even numbered clusters. This stability is explained on the basis of electron pairing effects [13, 15, 60]. With the same concept extended to complexes, we can say that complexes with even number of electrons are more stable. The maximum interaction energy is found to be for complex with Au_3. It is noticed that it also has the shortest anchoring bond with both the terminals (Fig. 1). The HOMO-LUMO gaps decrease on complexation. Figure 4 shows the HOMO-LUMO gaps for complexed and uncomplexed moieties. This might be due to the occupancy of the HOMO and LUMO orbitals by the cluster atoms. This effect may cause these complexes to behave as better conductors than uncomplexed proline.

As the size of the cluster increases, it is observed that there is hardly any increase in the E_{int} beyond Au_{10}. Complexes with 11–13 gold atoms show an almost equivalent amount of interaction and the corresponding anchoring bond lengths are also nearly same. Thus, we may conclude that beyond Au_{10} the electronic properties of these complexes do not vary much with the size of cluster, i.e., a saturation is reached.

Dipole moment and hyperpolarizability values

Table 2 also shows the dipole moment (μ) and first order hyperpolarizability (β) values for the complexes. We find higher μ for amine terminal interaction, indicating a higher

Table 1 Geometrical features of the optimized complexes

System	Site of interaction	Δ r (X-H)	Δν (X-H)	Angle[a] [in deg(°)]
Au_3	Amine	0.01(N-H)	89.27(N-H)	109.99
		0.01(N-C)	74.09(N-C)	
	Carboxyl	−0.05(C-O)	−326.14(C-O)	176.40
		0.02(O-H)	538.28(O-H)	
Au_4	Amine	0.01(N-H)	92.15(N-H)	109.97
		0.02(N-C)	75.26(N-C)	
	Carboxyl	−0.05(C-O)	−327.77(C-O)	171.35
		0.02(O-H)	532.00(O-H)	
Au_5	Amine	0.01(N-H)	91.71(N-H)	110.04
		0.01(N-C)	52.49(N-C)	
	Carboxyl	−0.04(C-O)	−319.48(C-O)	171.93
		0.02(O-H)	254.00(O-H)	
Au_6	Amine	0.01(N-H)	91.24(N-H)	111.49
		0.02(N-C)	56.82(N-C)	
	Carboxyl	−0.03(C-O)	−310.45(C-O)	152.00
		0.02(O-H)	498.57(O-H)	
Au_7	Amine	0.01(N-H)	91.18(N-H)	110.05
		0.02(N-C)	48.74(N-C)	
	Carboxyl	−0.05(C-O)	−319.20(C-O)	175.34
		0.02(O-H)	498.57(O-H)	
Au_8	Amine	0.01(N-H)	98.94(N-H)	110.94
		0.01(N-C)	54.80(N-C)	
	Carboxyl	−0.03(C-O)	−315.23(C-O)	127.80
		0.01(O-H)	191.40(O-H)	
Au_9	Amine	0.01(N-H)	87.02(N-H)	110.79
		0.01(N-C)	47.77(N-C)	
	Carboxyl[b]	−0.02(C = O)	63.97(C = O)	109.40
		0.01(O-H)	47.21(O-H)	
Au_{10}	Amine	0.01(N-H)	92.71(N-H)	110.82
		0.01(N-C)	35.35(N-C)	
	Carboxyl	−0.05(C-O)	−312.14(C-O)	104.32
		0.01(O-H)	296.37(O-H)	
Au_{11}	Amine	0.01(N-H)	110.14(N-H)	110.98
		0.01(N-C)	44.09(N-C)	
	Carboxyl	−0.05(C-O)	−320.74(C-O)	174.12
		0.02(O-H)	474.96(O-H)	
Au_{12}	Amine	0.01(N-H)	119.31(N-H)	110.89
		0.01(N-C)	31.76(N-C)	
	Carboxyl	−0.05(C-O)	−313.33(C-O)	164.42
		0.02(O-H)	294.63(O-H)	
Au_{13}	Amine	0.01(N-H)	118.73(N-H)	110.93
		0.01(N-C)	38.94(N-C)	
	Carboxyl	−0.05(C-O)	−320.31(C-O)	146.24
		0.02(O-H)	343.23(O-H)	

X-H corresponds to the bond of the active site with other atoms of the amino acid.$\Delta r = r_{complex} - r_{proline}$; $\Delta \nu = \nu_{proline} - \nu_{complex}$. The *negative value* of $\Delta \nu$ indicates a blue shift for the corresponding bond

[a] ∠*Cα*-N-H in the case of amine and ∠O-H-Au in the case of carboxyl terminal interaction

[b] ∠*Cα*-N-H in carboxyl terminal interaction

amount of charge transfer taking place from this end. The only exception to this is again Au_9 associated complex. Here we find a higher μ value when simultaneous interaction from both terminals is taking place. Earlier, we had seen that these complexes also have a higher interaction energy. Thus, we can conclude that charge transfer interactions are playing a major role in stabilizing these complexes. Hyperpolarizability values (β) show a rise (Fig. 5) which can be explained on the basis of the breakdown of the centrosymmetric character of the uncomplexed clusters. β is generally higher for complexes formed from the carboxyl terminal. The only exception to this is the complex with Au_5 where the values are the same for both ends and for Au_9 where the value is lower for a simultaneous interaction is taking place from amine and carboxyl terminal. An increase in the value of β is observed as the size of the cluster is increased upto Au_{10}, after which the values lie more or less in the same range. Higher values of β indicate that these complexes might possess good non linear optical properties.

Natural population analysis

Natural charges of the active site have been shown in Fig. 1. In some cases, especially the ones forming complex with odd numbered clusters, we find that the charges over the atoms of the anchoring bonds have opposite signs. This depicts the ionic nature of the anchoring bond. A careful observation indicates that the higher the ionic character, the higher the interaction energy (Table 2). Table 3 represents the charges over proline and gold cluster in both complexed and uncomplexed forms. The quantity $\Delta q_{cluster}$ indicates a gain of charge by the cluster, suggesting that the cluster oxidizes the coordinated amino acid. Figure 3 indicates the hybridization of the active site atoms. We see an increased sp^3 character of nitrogen. This is supported by the pyramidalization of the amine nitrogen on complexation. For the interaction from the carboxyl end, there is a decrease in the sp^2 character of O in the carbonyl (C = O) bond, indicating a decrease of charge from that center. However for C-OH bond, there is an increased sp^3 character of the hydroxyl O, indicating an increase of charge. This observation in turn supports the existence of a non-conventional hydrogen bond between cluster and proline where cluster is acting as a proton acceptor.

Natural bond orbital analysis

Natural bond orbital methods involve the expression of molecular properties in terms of a 'natural Lewis structure' (NLS) depiction of wave function [61]. NBO allows any aspect of wave function to be expressed in terms of Lewis

Table 2 Binding energies (E_{bind}), interaction energies (E_{int}), dipole moment (μ), hyperpolarizability (β), vertical electron affinity ($EA_{vertical}$), vertical ionization potential ($IP_{vertical}$) of various complexes

System	E_{bind} (kcal mol^{-1})	Site of interaction	E_{int} (kcal mol^{-1})	μ (Debye)	$\beta \times 10$–30 e.s.u	$EA_{vertical}$ (eV)	$IP_{vertical}$(eV)
Au_3	−25.93	Amine	−32.29	6.87	406.95	1.15	6.07
		Carboxyl	−22.06	3.28	606.03	1.72	6.70
Au_4	−51.21	Amine	−31.33	6.42	426.40	1.09	6.96
		Carboxyl	−20.55	3.12	647.37	1.51	7.34
Au_5	−43.40	Amine	−16.66	5.31	440.08	2.17	6.26
		Carboxyl	−12.64	4.28	440.08	2.49	6.97
Au_6	−65.54	Amine	−12.28	6.55	496.53	1.66	6.93
		Carboxyl	−6.00	2.50	765.41	1.87	7.59
Au_7	−22.90	Amine	−26.56	7.87	507.21	2.07	5.85
		Carboxyl	−16.76	3.70	810.43	2.43	6.25
Au_8	−56.52	Amine	−19.47	8.64	497.52	1.37	6.82
		Carboxyl	−8.89	2.95	765.38	1.69	7.30
Au_9	−32.55	Amine	−13.77	6.94	516.14	1.66	5.14
		Carboxyl	−15.88	12.38	336.54	1.79	5.56
Au_{10}	−59.64	Amine	−20.78	6.17	575.63	2.02	6.41
		Carboxyl	−7.54	3.21	894.84	2.67	6.89
Au_{11}	−39.93	Amine	−13.00	6.84	521.93	2.59	6.43
		Carboxyl	−10.48	3.89	833.658	2.80	5.49
Au_{12}	−53.57	Amine	−10.63	6.40	502.02	2.23	7.02
		Carboxyl	−3.55	4.41	928.54	2.59	6.12
Au_{13}	−46.66	Amine	−14.24	6.20	517.09	2.68	6.01
		Carboxyl	−8.77	3.97	957.87	3.08	5.63

(one-center lone-pair or two-center bond-pair) and non-Lewis type (all remaining orbitals) contributions, helping us to apply the elementary valence bond concepts to the modern wave functions. NBOs basically describe the residual resonance delocalization effects giving an insight to the existing inter- and intramolecualr interactions in the system.

Second-order perturbation theory analysis is done to evaluate the donor-acceptor interactions within the NBO framework. This gives a quantitative view of the charge transfer interactions existing between the donor and the acceptor species. These interactions result in a reduction of occupancy from the localized NBOs of the idealized Lewis structure into the empty non-Lewis orbitals. Table 4 shows the stabilization energy ($E^{(2)}$) values for the complexes. In general, we see greater $E^{(2)}$ values for complexes formed from the amine terminal which supports our previous results of higher interaction energy from the amine terminal (Table 2). Maximum $E^{(2)}$ value is noted for Au_4 complex. We observe that for the anchoring bonds, the lone pair of the donor (N,O) is transferred to the antibonding orbitals of the metal, but there is a backdonation of electron density from the cluster to the proline. Especially, the lonepairs of gold are found to donate the electrons to the antibonding orbital of the anchoring bonds. The HOMO orbitals lie on the metal and the LUMO orbitals for some cases are occupied by the metal cluster (even numbered clusters interacting from the carboxyl terminal), whereas, in other cases are centered on the carboxyl group indicating a charge transfer (Fig. 6). This results in the reduction of the HOMO-LUMO gaps for the complex (Fig. 4).

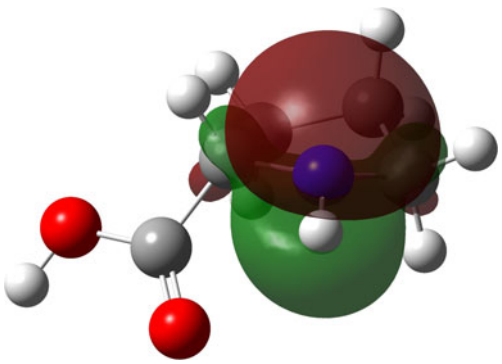

Fig. 2 The HOMO of proline generated by the NBO calculations

Atoms-in-molecules analysis

In AIM analysis, the nature of interaction is studied in terms of properties of electron density and its derivatives [62, 63].

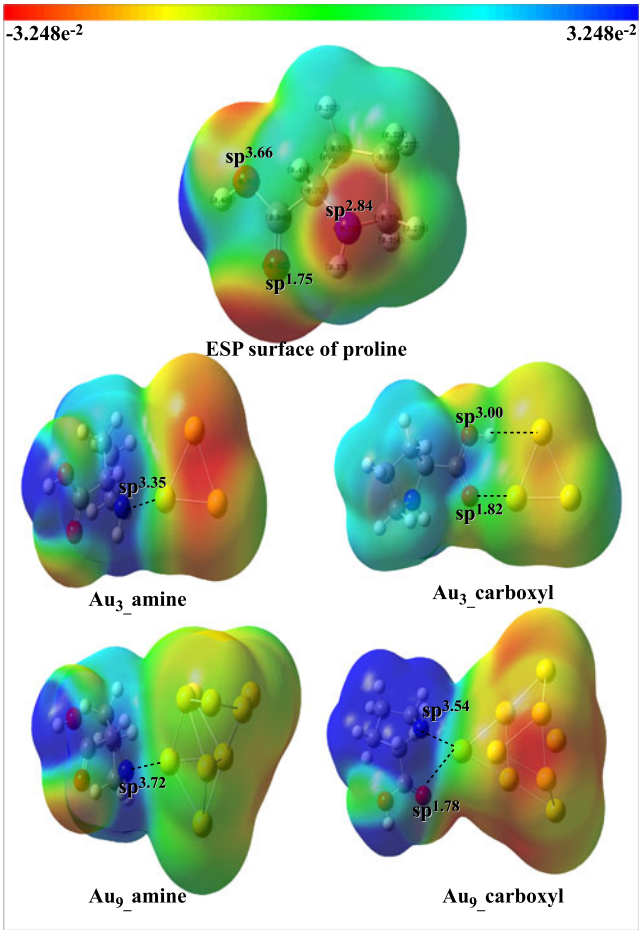

Fig. 3 Electrostatic potential mapped over isodensity surface for some selected species. The isovalue for these images is 0.0004 a.u

Table 5 shows some of the important parameters of AIM analysis. The term $\nabla^2 \rho$ (**r**) is related to bond interaction energy. A positive value represents a depletion of electronic charge density along the bond, a case of ionic interaction. A negative value indicates a charge density concentrated at the center of the inter nuclear region, a case of covalent interaction. Table 5 indicates a positive $\nabla^2 \rho$ (**r**) in all the cases, existence of ionic interaction is thus supported.

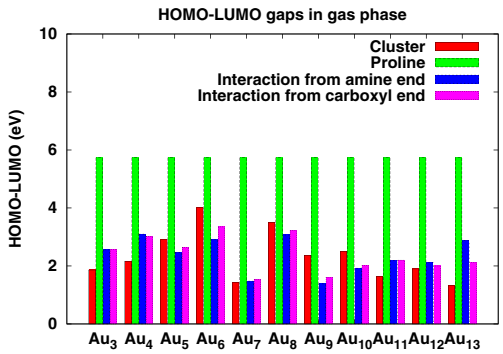

Fig. 4 HOMO-LUMO values in eV for both complexed and uncomplexed species

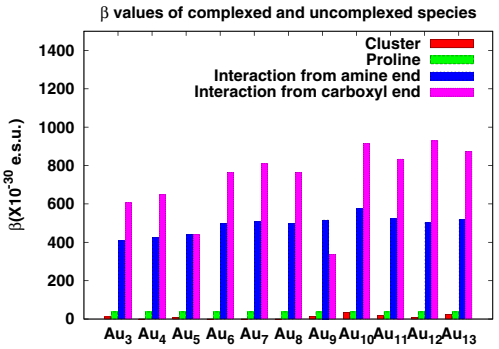

Fig. 5 Hyperpolarizability values for complexed and uncomplexed species

The electronic energy density, H(**r**), at the bond critical point (BCP) is given as:

$$H(\mathbf{r}) = G(\mathbf{r}) + V(\mathbf{r}), \tag{5}$$

where G(**r**) represents the kinetic energy density and V(**r**) the potential energy density. The negative H(**r**) indicates a stabilization effect due to accumulation of charge at **r**, as the case of covalent interaction. Table 5 indicates negative values for H(**r**) in most of the cases. The more negative H

Table 3 Natural population analysis indicating charge accepted/donated by the gold cluster

System	Site of interaction	$q_{cluster}$	$q_{cluster\text{-}complex}$	$\Delta q_{cluster}$
Au_3	Amine	0.001	−0.207	−0.206
	Carboxyl	0.001	−0.075	−0.074
Au_4	Amine	0.000	−0.232	−0.232
	Carboxyl	0.000	−0.095	−0.095
Au_5	Amine	0.000	−0.215	−0.215
	Carboxyl	0.000	−0.090	−0.090
Au_6	Amine	0.000	−0.183	−0.183
	Carboxyl	0.000	−0.073	−0.073
Au_7	Amine	0.000	−0.218	−0.218
	Carboxyl	0.000	−0.084	−0.084
Au_8	Amine	0.000	−0.184	−0.184
	Carboxyl	0.000	−0.133	−0.133
Au_9	Amine	0.000	−0.230	−0.230
	Carboxyl	0.000	−0.200	−0.200
Au_{10}	Amine	0.000	−0.231	−0.231
	Carboxyl	0.000	−0.187	−0.187
Au_{11}	Amine	0.000	−0.189	−0.189
	Carboxyl	0.000	−0.031	−0.031
Au_{12}	Amine	0.000	−0.174	−0.174
	Carboxyl	0.000	−0.126	−0.126
Au_{13}	Amine	0.000	−0.186	−0.186
	Carboxyl	0.000	−0.119	−0.119

$\Delta q_{cluster}$ here represents the charge gained or lost by the cluster when it forms complex with Pro

Table 4 Second order perturbation theory analysis of Fock matrix in NBO basis

System	Site of interaction	Donor NBO (i)	Acceptor NBO (j)	$E^{(2)}$ (kcal mol^{-1})
Au_3	Amine	$n_{A\mu 1}$	σ^*_{N4-Au2}	8.48
	Carboxyl	$n_{A\mu 1}$	$\sigma^*_{O19-H20}$	2.18
Au_4	Amine	$n_{A\mu 1}$	σ^*_{N5-Au3}	47.94
	Carboxyl	$n_{A\mu 4}$	$\sigma^*_{O20-H21}$	1.62
Au_5	Amine	$n_{A\mu 4}$	σ^*_{Au4-N6}	1.15
		$n_{A\mu 3}$	σ^*_{Au4-N6}	4.22
	Carboxyl	n_{o19}	$\sigma^*_{Au1-Au2}$	2.95
Au_6	Amine	$n_{A\mu 4}$	σ^*_{N7-C9}	23.86
	Carboxyl	$n_{A\mu 4}$	$\sigma^*_{C15-O20}$	5.38
Au_7	Amine	$n_{A\mu 4}$	σ^*_{Au1-N8}	3.91
		$n_{A\mu 4}$	$\sigma^*_{C13-H18}$	2.07
		$n_{A\mu 4}$	σ^*_{N8-H22}	3.48
	Carboxyl	$n_{A\mu 1}$	$\sigma^*_{C16-O21}$	5.46
		$n_{A\mu 2}$	$\sigma^*_{O23-H24}$	3.70
Au_8	Amine	$n_{A\mu 6}$	σ^*_{N9-C11}	15.04
	Carboxyl	$n_{A\mu 5}$	$\sigma^*_{O24-H25}$	1.15
Au_9	Amine	$n_{A\mu 7}$	$\sigma^*_{Au2-N10}$	18.98
	Carboxyl	$n_{A\mu 1}$	$\sigma^*_{C11-H13}$	1.79
Au_{10}	Amine	$n_{A\mu 9}$	$\sigma^*_{Au3-N11}$	19.20
	Carboxyl	$n_{A\mu 5}$	$\sigma^*_{O25-H26}$	1.46

(**r**), the greater the covalent character of the bond. We find that for complexes with higher interaction energy and shorter anchoring bond lengths, the H(**r**) is more negative. From this we can conclude that the anchoring bonds are partially ionic and partially covalent in nature. We also find that the value of H(**r**) for non-conventional hydrogen bond between Au and H of the carboxyl group is either very low or positive. Also, the H(**r**) is greater (in magnitude) for interaction from the amine terminal except Au_9 system, again supporting our previous conclusion of greater interaction from amine terminal.

Vertical ionization energies and electron affinity

Gold clusters have significantly larger electron affinities and ionization potentials than amino acids. Table 2 represents the vertical ionization potentials and electron affinities of all the complexes. Earlier works suggest that the electron and hole transfer phenomenon of molecules can be understood by investigating their electron affinities and ionization potentials [64, 65]. The electron affinity values lie in the range of 1–3 eV for all the complexes. These observations are in line with an earlier reported result of Shukla et al. where they have studied the cluster interaction with DNA base pairs [66]. The ionization potential values hardly change with increase in the size of the cluster.

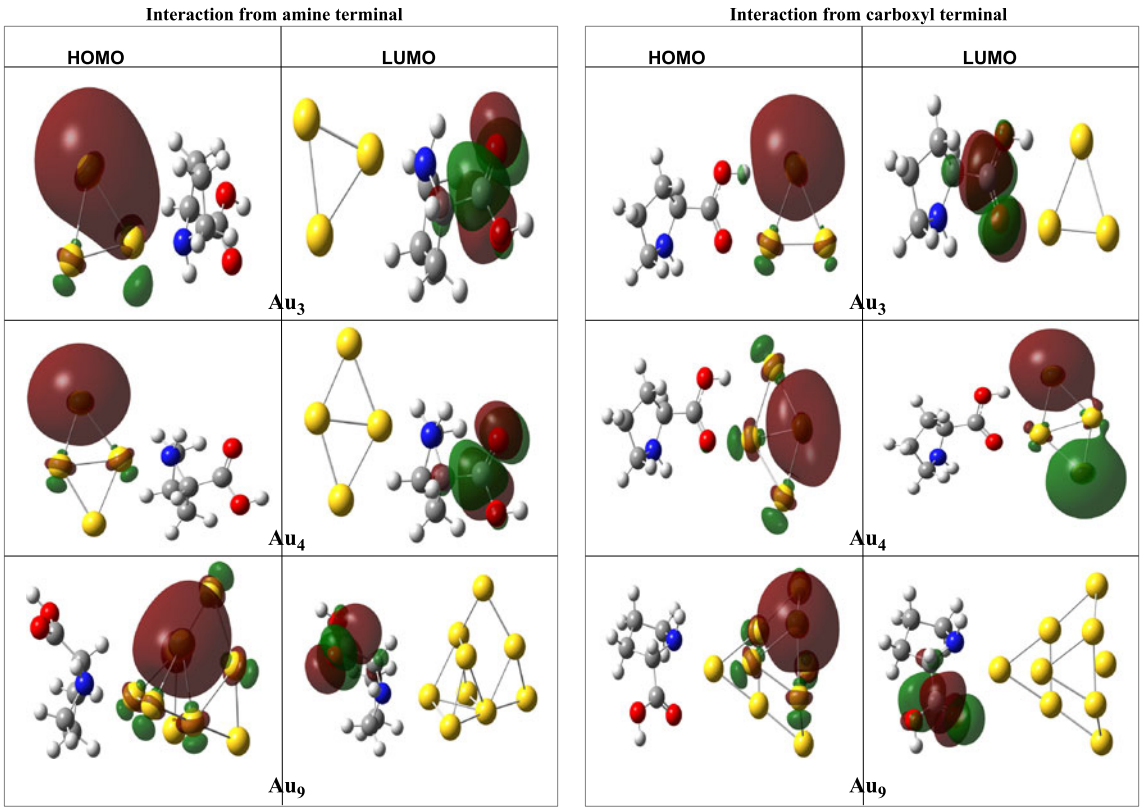

Fig. 6 HOMO and LUMO orbitals of some selected complexes

Table 5 Bond critical point data (in atomic units) from AIM analysis

System	Site of interaction	BCP	ρ	$\nabla^2\rho$	G(**r**)	V(**r**)	H(**r**)
Au_3	Amine	Au2 N4	9.20×10^{-2}	3.39×10^{-1}	1.08×10^{-1}	-1.32×10^{-1}	-0.24×10^{-1}
	Carboxyl	Au2 O17	7.20×10^{-2}	3.52×10^{-1}	9.61×10^{-2}	-1.04×10^{-1}	-0.08×10^{-1}
		Au1 H20	2.07×10^{-2}	4.52×10^{-2}	1.16×10^{-2}	-1.19×10^{-2}	-0.03×10^{-2}
Au_4	Amine	Au3 N5	9.14×10^{-2}	3.35×10^{-1}	1.07×10^{-1}	-1.31×10^{-1}	-0.24×10^{-1}
	Carboxyl	Au3 O18	7.08×10^{-2}	3.46×10^{-1}	9.40×10^{-2}	-1.02×10^{-1}	-0.08×10^{-1}
		Au4 H21	2.08×10^{-2}	4.46×10^{-2}	1.15×10^{-2}	-1.18×10^{-2}	-0.03×10^{-2}
Au_5	Amine	Au1 H10	1.19×10^{-2}	3.20×10^{-2}	7.36×10^{-3}	-6.76×10^{-3}	0.6×10^{-3}
		Au4 N6	7.97×10^{-2}	2.82×10^{-2}	8.80×10^{-2}	-1.05×10^{-1}	-0.17×10^{-1}
	Carboxyl	Au1 O19	5.79×10^{-2}	2.72×10^{-1}	7.19×10^{-2}	-7.60×10^{-2}	-0.41×10^{-2}
		Au1 H21	1.61×10^{-2}	4.40×10^{-2}	1.03×10^{-2}	-9.70×10^{-3}	0.06×10^{-2}
Au_6	Amine	Au4 N7	6.68×10^{-2}	2.41×10^{-1}	7.21×10^{-2}	-8.38×10^{-2}	-1.17×10^{-2}
		Au5 H17	7.57×10^{-3}	1.89×10^{-2}	4.31×10^{-3}	-3.90×10^{-3}	0.41×10^{-3}
	Carboxyl	Au4 O20	3.42×10^{-2}	1.45×10^{-1}	3.36×10^{-2}	-3.49×10^{-2}	-0.13×10^{-2}
		Au5 H22	1.73×10^{-2}	4.40×10^{-2}	1.05×10^{-2}	-1.00×10^{-2}	0.05×10^{-2}
Au_7	Amine	Au1 N8	8.57×10^{-2}	3.14×10^{-1}	9.90×10^{-2}	-1.19×10^{-1}	-0.20×10^{-1}
	Carboxyl	Au1 O21	6.35×10^{-2}	3.06×10^{-1}	8.19×10^{-2}	-8.73×10^{-2}	-0.54×10^{-2}
		Au2 H24	2.00×10^{-2}	4.21×10^{-2}	1.09×10^{-2}	-1.13×10^{-2}	-0.04×10^{-2}
Au_8	Amine	Au6 N9	7.84×10^{-2}	2.87×10^{-2}	8.87×10^{-2}	-1.06×10^{-1}	-0.17×10^{-1}
	Carboxyl	Au8 O22	4.55×10^{-2}	2.05×10^{-1}	5.24×10^{-2}	-5.34×10^{-2}	-0.10×10^{-2}
		Au8 H25	1.39×10^{-2}	3.80×10^{-2}	8.77×10^{-3}	-8.04×10^{-3}	0.73×10^{-3}
Au_9	Amine	Au2 N10	7.97×10^{-2}	2.92×10^{-1}	9.05×10^{-2}	-1.08×10^{-1}	-0.18×10^{-1}
	Carboxyl	Au5-N10	7.12×10^{-2}	2.65×10^{-1}	7.99×10^{-2}	-9.36×10^{-2}	-1.37×10^{-2}
		Au5 O23	2.60×10^{-2}	1.03×10^{-1}	2.47×10^{-1}	-2.36×10^{-1}	0.11×10^{-1}
Au_{10}	Amine	Au3 N11	8.06×10^{-2}	2.94×10^{-1}	9.16×10^{-2}	-1.10×10^{-1}	-0.18×10^{-1}
	Carboxyl	Au1 O25	8.39×10^{-2}	3.95×10^{-1}	1.11×10^{-1}	-1.24×10^{-1}	-0.13×10^{-1}
		Au4 O24	8.26×10^{-2}	3.90×10^{-1}	1.10×10^{-1}	-1.22×10^{-1}	-0.12×10^{-1}

An interesting observation comes out from the natural charge analysis of these anionic and cationic species. The extra charge resides over the gold cluster. Even when the electron is removed from the system, the charge over the cluster region is reduced. Hence, the cluster may act as a protective agent for the amino acid when it is subjected to a high energy/ionizing radiation. Also the HOMO for both cases lies on the metal cluster indicating that any electron exchange will be from the cluster part, not affecting the amino acid at all (Fig. S6 of supporting information).

Conclusions

Gold nanoclusters form stable complexes with proline. It is found that the interaction from the amine terminal is favored over the interaction from the carboxyl end which is also supported by the NBO and AIM data. The major bonding factors found to govern this interaction are the anchoring bonds between Au-N(O) and the non conventional hydrogen bonding between O-H···Au. The highest interaction energy is found for complex with Au_3. No specific trend for interaction energy is observed on increasing the size of the cluster. Reduced HOMO-LUMO gaps suggest that these complexes might behave as good conductors. Increased hyperpolarizability values indicate good non linear optical properties for these complexes. The AIM analysis indicates a partial ionic character for the anchoring bonds. NPA indicates that the cluster tends to oxidize the proline molecule. Second order perturbation analysis indicates the effective charge transfer existing in these complexes also supported by higher values of dipole moments. The computed values of vertical ionization potential and electron affinity indicate that gold clusters can also act as protective agents for the amino acid molecule in conditions of high/low charge densities.

Acknowledgments We thank the Department of Science and Technology, New Delhi, Government of India, for financial support. One of the authors (Sandhya Rai) acknowledges (Council of Scientific and Industrial Research Junior Research Fellowship) fellowship Via 20-12/2009(ii)EU-IV.

References

1. Parker JF, Fields-Zinna CA, Murray RW (2010) The story of a monodisperse gold nanoparticle: Au25l18. Acc Chem Res 43 (9):1289–1296
2. Li J, Li X, Zhai HJ, Wang LS (2003) Au20: a tetrahedral cluster. Science 299(5608):864–867
3. Woehrle GH, Warner MG, Hutchison JE (2002) Ligand exchange reactions yield subnanometer, thiol-stabilized gold particles with defined optical transitions. J Phys Chem B 106(39):9979–9981
4. Whetten RL, Shafigullin MN, Khoury JT, Schaaff TG, Vezmar I, Alvarez MM, Wilkinson A (1999) Crystal structures of molecular gold nanocrystal arrays. Acc Chem Res 32(5):397–406
5. Jin R, Cao Y, Mirkin CA, Kelly KL, Schatz GC, Zheng JG (2001) Photoinduced conversion of silver nanospheres to nanoprisms. Science 294(5548):1901–1903
6. Mirkin CA, Letsinger RL, Mucic RC, Storhoff JJ (1996) A DNA-based method for rationally assembling nanoparticles into macroscopic materials. Nature 382(6592):607–609
7. Chen XJ, Sanchez-Gaytan BL, Qian Z, Park SJ (2012) Noble metal nanoparticles in DNA detection and delivery. Nanomed Nanobiotech 4(3):273–290
8. Oldenburg SJ, Jackson JB, Westcott SL, Halas NJ (1999) Infrared extinction properties of gold nanoshells. Appl Phys Lett 75 (19):2897–2899
9. Shafai GS, Shetty S, Krishnamurty S, Shah V, Kanhere DG (2007) Density functional investigation of the interaction of acetone with small gold clusters. J Chem Phys 126(1):014704
10. Haruta M, Kobayashi T, Sano H, Yamada N (1987) Novel gold catalysts for the oxidation of carbon monoxide at a temperature far below 0 °C. Chem Lett 16(2):405–408
11. Lee TH, Ervin KM (1994) Reactions of copper group cluster anions with oxygen and carbon monoxide. J Phys Chem 98 (40):10,023–10,031
12. Garzón IL, Rovira C, Michaelian K, Beltrán MR, Ordejón P, Junquera J, Sánchez-Portal D, Artacho E, Soler JM (2000) Do thiols merely passivate gold nanoclusters? Phys Rev Lett 85:5250–5251
13. Häkkinen H, Moseler M, Landman U (2002) Bonding in Cu, Ag, and Au clusters: relativistic effects, trends, and surprises. Phys Rev Lett 89:033,401–033,404
14. Furche F, Ahlrichs R, Weis P, Jacob C, Gilb S, Bierweiler T, Kappes MM (2002) The structures of small gold cluster anions as determined by a combination of ion mobility measurements and density functional calculations. J Chem Phys 117(15):6982–6990
15. Pyykkö P (1988) Relativistic effects in structural chemistry. Chem Rev 88(3):563–594
16. Pyykkö P (2004) Theoretical chemistry of gold. Angew Chem Int Ed 43(34):4412–4456
17. Huang W, Wang LS (2009) Probing the 2d to 3d structural transition in gold cluster anions using argon tagging. Phys Rev Lett 102:153,401–153,404
18. Zhang L, Gu FX, Chan JM, Wang AZ, Langer RS, Farokhzad OC (2007) Nanoparticles in medicine: therapeutic applications and developments. Clin Pharmacol Ther 83:761–769
19. Chen P, Mwakwari S, Oyelere A (2008) Gold nanoparticles: from nanomedicine to nanosensing. Nanotech Sci Apps 1:45–66
20. De M, You CC, Srivastava S, Rotello VM (2007) Biomimetic interactions of proteins with functionalized nanoparticles: a thermodynamic study. J Am Chem Soc 129(35):10,747–10,753
21. Yu J, Choi S, Richards CI, Antoku Y, Dickson RM (2008) Live cell surface labeling with fluorescent ag nanocluster conjugatesâ€. Photochem Photobiol 84(6):1435–1439
22. Upert G, Bouillére F, Wennemers H (2012) Oligoprolines as scaffolds for the formation of silver nanoparticles in defined sizes: Correlating molecular and nanoscopic dimensions. Angew Chem Int Ed 51(17):4231–4234
23. Tabarin T, Kulesza A, Antoine R, Mitrić R, Broyer M, Dugourd P, Bonačić Koutecký V (2008) Absorption enhancement and conformational control of peptides by small silver clusters. Phys Rev Lett 101:213001–213005
24. Bonačić Koutecký V, Kulesza A, Gell L, Mitrić R, Antoine R, Bertorelle F, Hamouda R, Rayane D, Broyer M, Tabarin T, Dugourd P (2012) Silver cluster-biomolecule hybrids: from basics towards sensors. Phys Chem Chem Phys 14:9282–9290
25. West JL, Halas NJ (2003) Engineered nanomaterials for biophotonics applications: improving sensing, imaging, and therapeutics. Annu Rev Biomed Eng 5(1):285–292
26. Pal S, Mitra K, Azmi S, Ghosh JK, Chakraborty TK (2011) Towards the synthesis of sugar amino acid containing antimicrobial noncytotoxic cap conjugates with gold nanoparticles and a mechanistic study of cell disruption. Org Biomol Chem 9:4806–4810
27. Burda C, Chen X, Narayanan R, El-Sayed MA (2005) Chemistry and properties of nanocrystals of different shapes. ChemInform 36 (27):1025–1102
28. Katz E, Willner I (2004) Integrated nanoparticle biomolecule hybrid systems: synthesis, properties, and applications. Angew Chem Int Ed 43(45):6042–6108
29. Terawaki A, Otsuka Y, Lee H, Matsumoto T, Tanaka H, Kawai T (2005) Conductance measurement of a DNA network in nanoscale by point contact current imaging atomic force microscopy. Appl Phys Lett 86(11):113,901–113,903
30. Rodriguez-Vazquez MJ, Blanco MC, Lourido R, Vazquez-Vazquez C, Pastor E, Planes GA, Rivas J, Lopez-Quintela MA (2008) Synthesis of atomic gold clusters with strong electrocatalytic activities. Langmuir 24(21):12,690–12,694
31. Antoine R, Bertorelle F, Broyer M, Compagnon I, Dugourd P, Kulesza A, Mitrić R, Bonačić Koutecký V (2009) Gas-phase synthesis and intense visible absorption of tryptophanâ€ gold cations. Angew Chem Int Ed 48(42):7829–7832
32. Lynch I, Dawson KA (2008) Protein-nanoparticle interactions. Nano Today 3(12):40–47
33. Hayat MA (ed) (1989) Colloidal gold: principles, methods, and applications, 1st edn. Academic, New York
34. Saha K, Agasti SS, Kim C, Li X, Rotello VM (2012) Gold nanoparticles in chemical and biological sensing. Chem Rev 112 (5):2739–2779
35. Krishnan N, Dickman MB, Becker DF (2008) Proline modulates the intracellular redox environment and protects mammalian cells against oxidative stress. Free Radic Biol Med 44(4):671–681
36. Lang F (2007) Mechanisms and significance of cell volume regulation. J Am Coll Nutr 26(suppl 5):613S–623S
37. Zhao Y, Truhlar DG (2005) How well can new-generation density functional methods describe stacking interactions in biological systems? Phys Chem Chem Phys 7:2701–2705
38. Zhao Y, Truhlar DG (2007) Density functionals for noncovalent interaction energies of biological importance. J Chem Theor Comput 3(1):289–300
39. Knal A, Acar N (2010) A DFT and TD-DFT study on intermolecular charge transfer complexes of pyrene with phenothiazine and promazine. J Mol Str THEOCHEM 949(13):36–40
40. Fernández EM, Soler JM, Garzón IL, Balbás LC (2004) Trends in the structure and bonding of noble metal clusters. Phys Rev B 70:165,403
41. Perdew JP, Burke K, Ernzerhof M (1996) Generalized gradient approximation made simple. Phys Rev Lett 77:3865–3868
42. Tao J, Perdew JP, Staroverov VN, Scuseria GE (2003) Climbing the density functional ladder: nonempirical meta-generalized gradient approximation designed for molecules and solids. Phys Rev Lett 91(14):146401

43. Ehlers A, Bhme M, Dapprich S, Gobbi A, Hllwarth A, Jonas V, Khler K, Stegmann R, Veldkamp A, Frenking G (1993) A set of f-polarization functions for pseudo-potential basis sets of the transition metals ScCu, YAg and LaAu. Chem Phys Lett 208(12):111–114
44. Dolg M, Wedig U, Stoll H, Preuss H (1987) Energy-adjusted ab initio pseudopotentials for the first row transition elements. J Chem Phys 86(2):866–872
45. Andrae D, Huermann U, Dolg M, Stoll H, Preu H (1990) Energy-adjusted ab-initio pseudopotentials for the second and third row transition elements. Theor Chim Acta 77:123–141
46. Fernández EM, Soler JM, Balbás LC (2006) Planar and cagelike structures of gold clusters: density-functional pseudopotential calculations. Phys Rev B 73:235,433
47. Hariharan P, Pople J (1974) Accuracy of AH_n equilibrium geometries by single determinant molecular orbital theory. Mol Phys 27 (1):209–214
48. Hariharan P, Pople J (1972) The effect of d-functions on molecular orbital energies for hydrocarbons. Chem Phys Lett 16(2):217–219
49. Rassolov VA, Ratner MA, Pople JA, Redfern PC, Curtiss LA (2001) 6–31 G* basis set for third-row atoms. J Comput Chem 22(9):976–984
50. Hehre WJ, Ditchfield R, Pople JA (1972) Self—consistent molecular orbital methods. xii. further extensions of gaussian—type basis sets for use in molecular orbital studies of organic molecules. J Chem Phys 56(5):2257–2261
51. Dennington R, Keith T, Millam J (2009) GaussView Version 5. Semichem Inc. Shawnee Mission, KS
52. Glendening ED, Reed AE, Carpenter JE, Weinhold F (2004) NBO Version 3.1. Gaussian, Inc., Wallingford, CT
53. Weinhold F, Landis CR (2001) Natural bond orbitals and extensions of localized bonding concepts. Chem Educ Res Pract 2:91–104
54. Todd A Keith TG (2012) AIMAll (version 12.09.23). Overland Park, KS
55. Frisch MJ, Trucks GW, Schlegel HB, Scuseria GE, Robb MA, Cheeseman JR, Scalmani G, Barone V, Mennucci B, Petersson GA, Nakatsuji H, Caricato M, Li X, Hratchian HP, Izmaylov AF, Bloino J, Zheng G, Sonnenberg JL, Hada M, Ehara M, Toyota K, Fukuda R, Hasegawa J, Ishida M, Nakajima T, Honda Y, Kitao O, Nakai H, Vreven T, Montgomery JA Jr, Peralta JE, Ogliaro F, Bearpark M, Heyd JJ, Brothers E, Kudin KN, Staroverov VN, Kobayashi R, Normand J, Raghavachari K, Rendell A, Burant JC, Iyengar SS, Tomasi J, Cossi M, Rega N, Millam JM, Klene M, Knox JE, Cross JB, Bakken V, Adamo C, Jaramillo J, Gomperts R, Stratmann RE, Yazyev O, Austin AJ, Cammi R, Pomelli C, Ochterski JW, Martin RL, Morokuma K, Zakrzewski VG, Voth GA, Salvador P, Dannenberg JJ, Dapprich S, Daniels AD, Farkas O, Foresman JB, Ortiz JV, Cioslowski J, Fox DJ (2009) Gaussian 09 revision C.01. Gaussian Inc, Wallingford, CT
56. Gimeno MC (2009) The chemistry of gold. Wiley-VCH,Weinheim, pp 1–63
57. Pakiari AH, Jamshidi Z (2007) Interaction of amino acids with gold and silver clusters. J Phys Chem A 111(20):4391–4396
58. Joshi P, Shewale V, Pandey R, Shanker V, Hussain S, Karna SP (2011) Tryptophan gold nanoparticle interaction: a first-principles quantum mechanical study. J Phys Chem C 115(46):22,818–22,826
59. Xie HJ, Lei QF, Fang WJ (2012) Intermolecular interactions between gold clusters and selected amino acids cysteine and glycine: a DFT study. J Mol Model 18:645–652
60. Pyykkö P (2008) Theoretical chemistry of gold. iii. Chem Soc Rev 37:1967–1997
61. Glendening ED, Landis CR, Weinhold F (2012) Natural bond orbital methods. Comput Mol Sci 2(1):1–42
62. Bader RFW (1990) Atoms in molecules, 1st edn. Oxford University Press, Oxford
63. Bader R, Keith T, Gough K, Laidig K (1992) Properties of atoms in molecules: additivity and transferability of group polarizabilities. Mol Phys 75(5):1167–1189
64. Richardson NA, Wesolowski SS, Schaefer HF (2002) Electron affinity of the guaninecytosine base pair and structural perturbations upon anion formation. J Am Chem Soc 124(34):10,163–10,170
65. Crespo-Hernndez CE, Close DM, Gorb L, Leszczynski J (2007) Determination of redox potentials for the WatsonCrick base pairs, DNA nucleosides, and relevant nucleoside analogues. J Phys Chem B 111(19):5386–5395
66. Shukla MK, Dubey M, Zakar E, Leszczynski J (2009) DFT investigation of the interaction of gold nanoclusters with nucleic acid base guanine and the watson crick guanine-cytosine base pair. J Phys Chem C 113(10):3960–3966